Journal of Applied Polymer Science

Development of polyvinyl alcohol/intercalated MMT composite foams fabricated by melt extrusion

Yan Li,[1,2] Huafeng Tian,[1,2] Qingqing Jia,[1,2] Ping Niu,[3] Aimin Xiang,[1,2] Di Liu,[1,2] Yanan Qin[1,2]

[1]School of Material and Mechanical Engineering, Beijing Technology and Business University, Beijing 100048, China

[2]Key Laboratory of Carbohydrate and Biotechnology Ministry of Education, Jiangnan University, Lihu Road 1800, Wuxi 214122, China

[3]Exchange, Development and Service Center for Science and Technology Talents, MOST, People's Republic of China

Correspondence to: A. Xiang (E-mail: xaming@th.btbu.edu.cn) and H. Tian (E-mail: tianhuafeng@th.btbu.edu.cn)

ABSTRACT: In this work, novel polyvinyl alcohol (PVA)/intercalated montmorillonite (MMT) nanocomposite foams were fabricated by melt extrusion with fixed amount of foaming agent, and the structure and properties were investigated with X-ray diffraction, transmittance electron microscope, differential scanning calorimetry, plate rheometer, scanning electron microscope, density analysis, and mechanical testing in detail. The results revealed that pristine MMT could be intercalated by PVA during melt-extrusion. Both exfoliation and intercalation structure was formed in the composites. The strong interaction between PVA and MMT restricted the motion of PVA molecules, leading to the enhanced complex viscosity, storage modulus, and melt flow index, suggesting the improved melt elasticity and melt strength. The improved melt strength of PVA through MMT incorporation facilitated the foaming process. With the increase of MMT, cell rupture was limited and the thickness of cell-wall decreased, leading to the decreased density. The homogeneous cells and the closed cell structure with the foaming density of 0.35 g/cm^3 could be formed with 2 wt % MMT incorporation. With the increase of MMT, the tensile strength of PVA/MMT foams decreased because of the enlarged foaming ratio and decreased density. This work aims to pave a simple and convenient way to produce biodegradable foams. © 2015 Wiley Periodicals, Inc. J. Appl. Polym. Sci. **2015**, *132*, 42706.

KEYWORDS: biodegradable; clay; extrusion; foams

Received 26 November 2014; accepted 4 July 2015

DOI: 10.1002/app.42706

INTRODUCTION

Plastic foams are widely used in packaging, transportation, daily necessities, etc, for its unique characteristic such as low density, heat-insulation as well as low cost.[1,2] Polyvinyl alcohol (PVA) is a kind of water soluble polymers.[3,4] For its environmental friendly, antistatic and biocompatible character, PVA foams possess wide applications in packaging, water treatment, heavy metal adsorption, biomedicine and heat/sound insulation,[5,6] etc.

As a result of the strong hydrogen bonding between –OH groups on PVA, the melting temperature of PVA is close to its decomposition temperature. Therefore, the melting processing of PVA is difficult.[7,8] The common method for processing PVA foams is solution foaming[9] and molding foaming,[10] while the complex process and high cost limits the wild application of PVA foams. Melting extrusion is a convenient way to prepare polymeric foams, for example, PVA foams was prepared through melt extrusion with water as plasticizer in the presence of foaming agent.[11] However, water plasticizer is highly volatile in all these processes, leading to the unstable quality of the resulting PVA foams, which limit their application. The melt extrusion processing of PVA foams without water have not been reported until now.

In recent years, montmorillonite (MMT) has attracted great interest because of its high aspect ratio and specific surface area, leading to the wide applications in the field of polymeric composite materials.[12,13] With a small amount of MMT (<10 wt %), composites often show unexpectedly great improvement of properties compared with neat polymers or conventional composites.[14] For example, the water resistance,[15] thermal stability[16] besides the mechanical properties of PVA films could be dramatically improved by MMT.[17,18] However, the influence of MMT on the foaming properties of PVA has not been studied yet.

In our previous work,[19,20] the melt processing of PVA without water was successfully investigated, and the plasticized PVA could be extruded and blow molded. In this work, the PVA/MMT nanocomposites were processed by melt intercalation and the nanocomposite foams were prepared via melt-extrusion in presence of

constant amount of chemical foaming agent. The dependence of the morphology, density as well as the mechanical properties of the resulting foams with MMT content was investigated in detail. This work aims to analyze the mechanism that MMT improved the foaming process of PVA and pave a convenient and easy way to prepare environment friendly PVA foams with high performance.

MATERIALS AND METHODS

Materials

PVA (117) with the viscosity of 25.0–31.0×10^{-3} Pa·S and alcoholysis degree of 98.0–99.0 mol % was purchased from Kuraray. (Japan). Polyol plasticizers and azodicarbonamide (AC) chemical foaming agent of analytical grade were supplied by the Shanghai Chemical (Shanghai, China). Pristine Na^+-montmorillonite (PGW) was supplied by Nanocor (USA).

Preparation of PVA/MMT Composite Foams

The compound polyol plasticizers were prepared by mixing sorbitol and pentaerythritol with a ratio of 1 : 1. PVA, polyol plasticizers, and MMT with different weight ratios were first mixed in the high speed mixer. The mixtures were extruded by co-rotating twin-screw extruder at 220°C with a screw speed of 50 rpm. Thus the PVA/MMT composite materials were obtained. Then, with the incorporation of AC foaming agent (1%), PVA/MMT composites were prepared using a single-screw extruder at 220°C (screw temperature) and 210°C (die temperature) with a screw speed of 25 rpm. The PVA/MMT foams with different compositions were obtained.

Characterization

X-ray diffraction (XRD) patterns of the samples were recorded on a XRD instrument (XRD-6000, Shimadzu, Japan) with Cu $K\alpha$ radiation ($\lambda = 0.154$ nm) at 40 kV and 30 mA. X-ray diffraction data were collected from $2\theta = 1.5°$ to 10° at a scanning rate of 2°/min.

The structure and morphology of the nanocomposite powders and plastics were visualized by a transmittance electron microscope [TEM F30, FEI TECNAI, Netherlands] at an accelerating voltage of 200 kV. Ultrathin sections of the composites were prepared using a Leica Ultracut UCT with EMFCS cryo-attachment at −120°C. The cross-sections were obtained by using a diamond knife. The ultrathin films of the samples were directly placed on the copper grids and observed after sputtering carbon.

The crystallization behavior was analyzed using a differential scanning calorimeter analyzer (DSC Q100, TA Instruments, USA) under N_2 atmosphere. Samples of 3–5 mg were maintained at 240°C for 3 min to eliminate thermal history, and then the samples were cooled to 140°C with the cooling rate of 10°C/min to obtain the crystallization curves. The relative crystallinity X_t at certain temperature T was calculated by

$$X_t = \frac{\int_{T_0}^{T} (dH/dT)dT}{\int_{T_0}^{T_\infty} (dH/dT)dT} \quad (1)$$

where H is the crystallization enthalpy.

The nonisothermal crystallization of polymers can be described by Avrami equation,[21] which assumed that the relative degree of crystallinity developed with crystallization time t:

$$1 - X(t) = \exp(-Z_t t^n) \quad (2)$$

where $X(t)$ is the relative degree of crystallinity at certain time t, Z_t is a constant reflecting nonisothermal crystallization rate, and exponent n is a mechanism constant depending on the type nucleation and growth process. Using eq. (2) in double-logarithmic form:

$$\lg\{-\ln[1 - X(t)]\} = \lg Z_t + n \lg t \quad (3)$$

With data at low degree of crystallinity used in the linear regression, the values of n and $\lg Z_t$ were calculated from the slope and intercept of these plots. Jeziorny presented a modified form of Z_t, Z_c, which was dependent of cooling rate Φ:[22]

$$\ln Z_c = \frac{\ln Z_t}{\phi} \quad (4)$$

The half crystallization time $t_{1/2}$ is related to Z_c as

$$t_{1/2} = \left(\frac{\ln 2}{Z_c}\right)^{1/n} \quad (5)$$

The rheological properties of PVA/MMT composites measured in dynamic mode at 220°C using a rotational rheometer (ARES Rheometer, TA, USA) with a parallel plates (20 mm in diameter with a gap of 1.0 mm). The frequency range was 0.1–100 rad/s, and the maximum strain was fixed at 0.5%, to ensure that these analyses were within the linear viscoelastic region under nitrogen.

MFI measurements were carried out in a MP600 Extrusion Plastometer (Tinius Olsen, USA). Samples of approximately 5 g in mass were preheated for 200 seconds at 210°C for the composite in the barrel. The samples were then extruded through the die (2.096 mm × 8.001 mm) under a constant load of 2.16 kg.

The cell morphology was observed by the scanning electron microscope (SEM Tescan Vege II, Tescan SRO Instruments) under high vacuum. The foams in the dry state were frozen in liquid nitrogen, snapped immediately, and then vacuum-dried. The fractured surfaces were sputtered with gold before the SEM observation.

The density of the foams was determined using density type analyzer (Ultrapyc 1200e, Quantachrome Instruments, USA).

The tensile property was characterized by the mechanical testing machine (CMT6101, Shenzhen Sans Materials Testing) in tensile mode according to the GB/T 1040.3–2006 at 25°C with the testing speed of 10 mm/min. Mechanical tensile data were averaged over at least five specimens.

RESULTS AND DISCUSSION

Dispersion of MMT

The structural interlayer spacing of the PVA/MMT nanocomposites prepared via melting intercalation was investigated by X-ray diffraction. Figure 1 shows the XRD patterns of MMT, neat PVA, and the nanocomposites. The basal spacing of pristine MMT was calculated to be 1.20 nm from the diffraction peak at 7.38° using Bragg function. PVA displayed no obvious

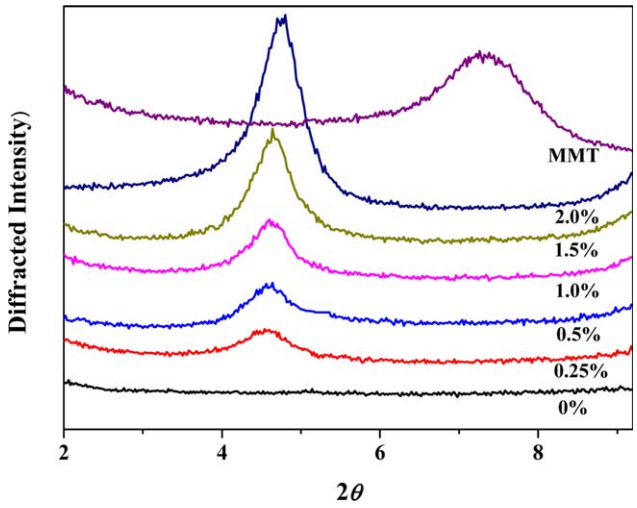

Figure 1. XRD curves of MMT and PVA/MMT composites. The MMT content was indicated in the figure. [Color figure can be viewed in the online issue, which is available at wileyonlinelibrary.com.]

crystallization peaks under the tested 2θ range. In the case of PVA/MMT composites with various MMT content, XRD patterns revealed sharp diffraction peaks at around 4.6° with the *d*-spacing values of about 1.92 nm. It indicated that the PVA macromolecules were inserted into the gallery of MMT layers, and the intercalated structure had been successfully prepared via melting intercalation process. With the increase of MMT loading, the degree of intercalated MMT increased, leading to the increased diffraction intensity, while the 2θ values of diffraction peaks almost unchanged.

TEM images of PVA/MMT composites with 1.0% (a) and 2.0% (b) MMT are shown in Figure 2. MMT layers were well dispersed in the PVA matrix. Some of MMT were exfoliated into randomized nanolayers. While other MMT layers still retained their orientation to some degree, and the MMT tactoids are highly delaminated into some thin lamellas by PVA molecules with a dimension of about 1–2 nm in thickness, indicating the intercalation. The difference between the two samples was that the exfoliation structure decreased and intercalation increased with the increase of MMT. The results from TEM were in agreement with that from XRD. PVA macromolecules could insert into the intercalated clay layers of MMT during melt processing, resulting in the highly delaminated or intercalated structure.

Nonisothermal Crystallization Analysis

The DSC curves for PVA/MMT composites with various MMT contents are shown in Figure 3 and the crystallization parameters are listed in Table I. Strong crystallization peaks of PVA at about 180°C were observed for all the composites tested. With the increase of MMT, both the onset crystallization and the crystallization peak temperature increased. During the crystallization process of PVA, the intercalated MMT layers might have acted as nucleating agent inducing crystallinity. Also, after the inserting of PVA molecules into the gallery of MMT, the affinity between PVA and MMT would limit the rearranging of PVA macromolecules into crystal lattice and hinder the crystallization of PVA. The crystallization temperature increased after incorporation of MMT.

The relationship between the relative crystallinity X_t and temperature T is shown in Figure 4. With the decrease of temperature, the crystallization process gradually completed. Acting as the nucleating agent, MMT could promote the crystallizing process. Therefore, the degree of crystallization of PVA/MMT composites was higher than that of neat PVA during the testing temperature.

The plots of $\lg\{-\ln[1-X(t)]\}$ as a function of $\lg t$ were drawn for all compositions, as shown in Figure 5. The related parameters are listed in Table I. With the increase of MMT, Z_c increased, suggesting the crystallization was completed rapidly. The values of n for PVA/MMT composites were larger than that of neat PVA at the same cooling rate, indicating that the MMT acts as a nucleating agent for PVA, which was in accordance with the analysis of DSC. The value of $t_{1/2}$ decreased with the incorporation of MMT, indicating that the crystallization process was accelerated and became easy.

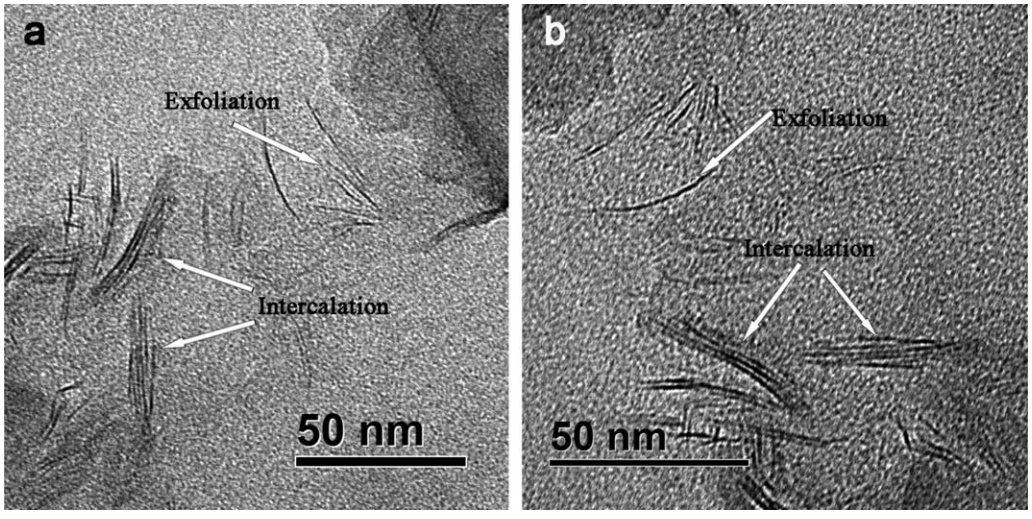

Figure 2. TEM images for PVA/MMT composites with (a) 1.0% and (b) 2.0% MMT.

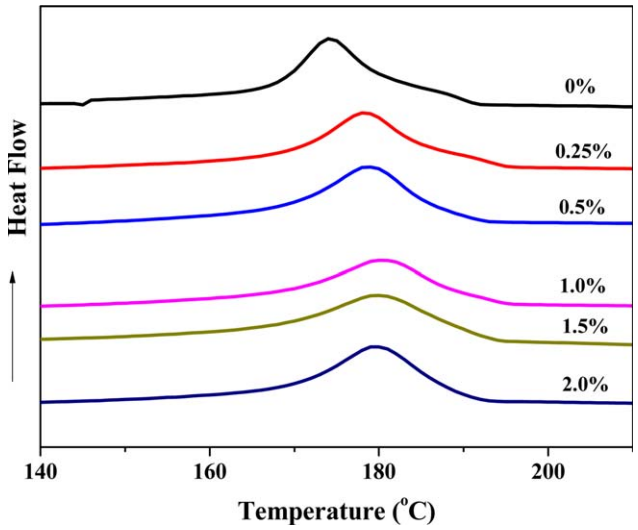

Figure 3. DSC curves of PVA/MMT composites with different amount of MMT. [Color figure can be viewed in the online issue, which is available at wileyonlinelibrary.com.]

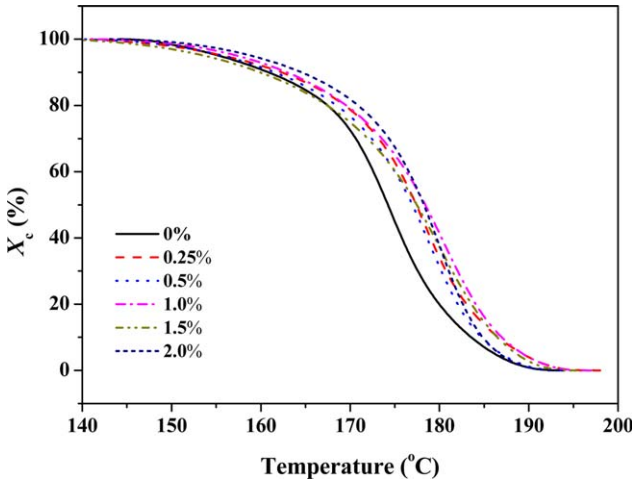

Figure 4. Dependence of relative crystallinity on temperature for PVA/MMT composites. [Color figure can be viewed in the online issue, which is available at wileyonlinelibrary.com.]

Rheological Behavior of PVA/MMT Composites

The melt strength of a polymer generally depends on the viscosity, dynamic storage modulus, and loss modulus. Rheological measurements were employed to evaluate the viscoelastic properties of PVA/MMT composites, as shown in Figures 6–8. The complex viscosity of PVA and PVA/MMT composites is shown in Figure 6. At low frequency, neat PVA exhibited as Newtonian fluid with viscosity almost unchanged. The phenomenon became weak after the incorporation of MMT. With the increase of shear frequency, the viscosity decreased for all the samples tested indicating a shear-thinning behavior. In the high frequency range, PVA molecules disentangled and orientated along the shearing direction, leading to the decreased flow resistance and viscosity. With the incorporation of MMT into PVA matrix, the complex viscosity of the composites increased compared with neat PVA. As discussed in the XRD analysis, the layered MMT was intercalated by the PVA macromolecules. Therefore, strong interaction such as hydrogen bonding would occur between PVA and MMT, leading to the reduced mobility of PVA macromolecule segments and hence increased viscosity. The shear force tested could not destroy the strong interactions between PVA and MMT, leading to the higher viscosity of the composites.

Table I. The Onset Crystallization ($T_{c\text{-onset}}$), the Crystallization Peak (T_{cp}) Temperature and the Kinetics Data Calculated by Avrami Method of PVA/MMT Composites

MMT content (wt %)	$T_{c\text{-onset}}$ (°C)	T_{cp} (°C)	n	Z_c	$t_{1/2}$ (min)
0	189.88	174.14	2.67	0.76	2.12
0.25	190.98	178.27	2.96	0.79	1.95
0.5	191.66	178.55	3.09	0.80	1.89
1.0	191.93	180.03	2.85	0.81	1.87
1.5	191.87	179.58	2.65	0.82	1.82
2.0	189.89	179.49	2.98	0.84	1.58

For polymers with high melt strength the foaming process would be facilitated. The melt strength could be characterized by the melt elasticity, which could be enhanced with the increase of shear storage modulus in the low frequency range.[23] As shown in Figure 7, the storage modulus as well as loss modulus of PVA/MMT composites increased obviously with the increase of MMT. As a result of the affinity between PVA and MMT and motion limitation of the MMT layer on PVA molecules, the slack time of PVA/MMT composites was longer than that of the neat PVA. The PVA molecules of composites did not have enough time to disentangle, resulting in the increased storage modulus. Therefore, with the increase of MMT, the storage modulus increased, leading to the enhanced melt strength.

Figure 8 shows the loss modulus of PVA/MMT composites with different MMT content. The loss modulus of the composites exhibited similar trends with the storage modulus and increased

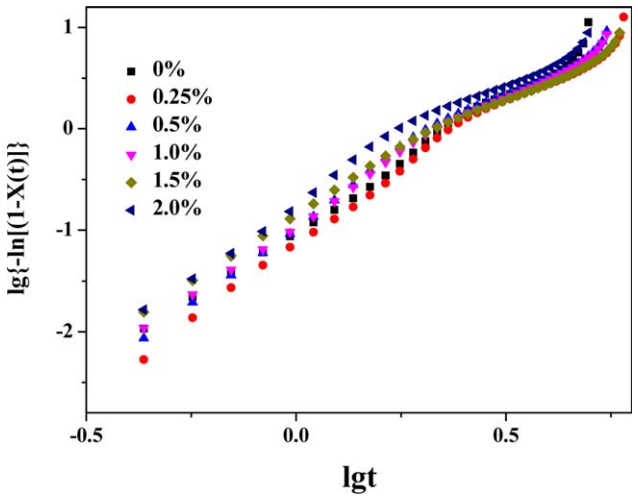

Figure 5. The Avrami curves of PVA/MMT composites. [Color figure can be viewed in the online issue, which is available at wileyonlinelibrary.com.]

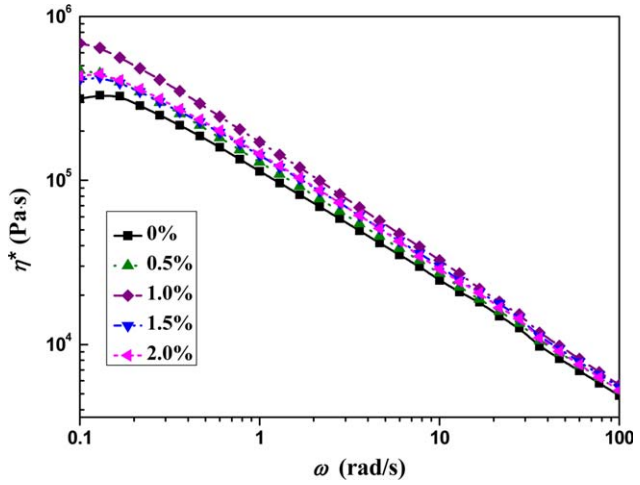

Figure 6. Complex viscosity of PVA/MMT composites. [Color figure can be viewed in the online issue, which is available at wileyonlinelibrary.com.]

with the increase of MMT. However, the amplification or changes of G'' was smaller than that of G', indicating that increment of elastic component of PVA/MMT composite melt was greater than that of the viscous component resulted from the interactions between the filler and matrix.

Melt flow index is also used to characterize the viscosity and melt strength of polymer melts. The lower melt index suggests higher viscosity and melt strength. Figure 9 shows the melt index for PVA/MMT composites with different content of MMT. With the increase of MMT, the melt index of PVA/MMT composites decreased linearly. PVA macromolecules could insert into the nanolayers of MMT after melt processing as indicated by XRD analysis. Also the interactions between PVA and MMT nanolayers could restrict the motion of PVA molecular chains, resulting in the increased melt index and melt viscosity.

It is interesting that both the viscosity and storage modulus exhibited the highest value at about 1% MMT content. The

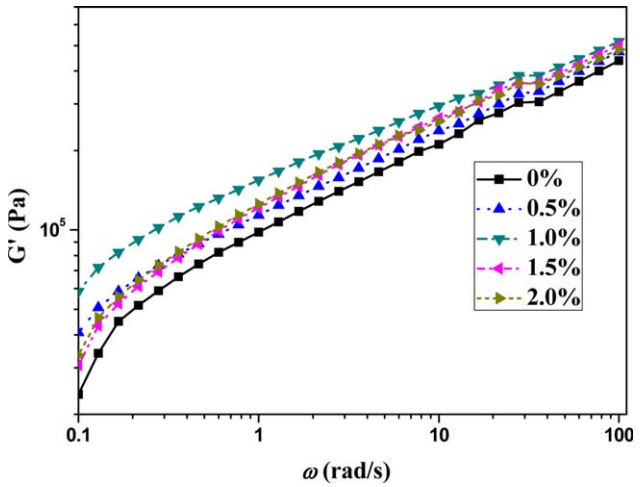

Figure 7. Storage modulus of PVA/MMT composites. [Color figure can be viewed in the online issue, which is available at wileyonlinelibrary.com.]

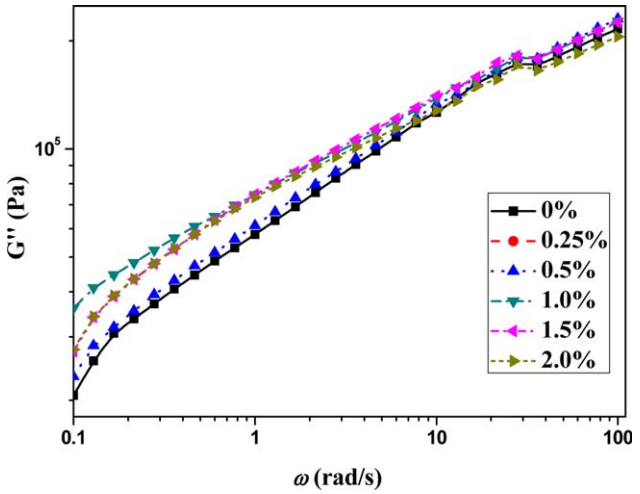

Figure 8. Loss modulus of PVA/MMT composites. [Color figure can be viewed in the online issue, which is available at wileyonlinelibrary.com.]

decrease of melt index also became mild with MMT content more than 1.0%. The reason may be that the exfoliation may decreased and intercalation increased with the increase of MMT as indicated in the TEM images, resulting the decreased reinforcing effect of MMT on PVA matrix.

Cell Morphology of PVA/MMT Composite Foams

The morphology of neat PVA foam and PVA/MMT composite foams prepared with the same amount of foaming agent (1%) is shown in Figure 10. Serious cell coalescence and rupture occurred in neat PVA matrix [Figure 10(a)]. During the foaming process, the cell wall ruptured and coalescence occurred for the low melt strength of neat PVA, resulting in the leakage of the gas and low foaming ratio. For PVA/MMT composite foams, the phenomenon of cell coalescence and rupture was limited, and the cell size became more uniform with the thinner cell-wall with the increase of MMT. The result shows that MMT could facilitate the foaming process. As discussed above, the melt strength of PVA increased with the addition of MMT. The generated gas could grow sufficiently in the melt, and with the increase of the melt strength, the

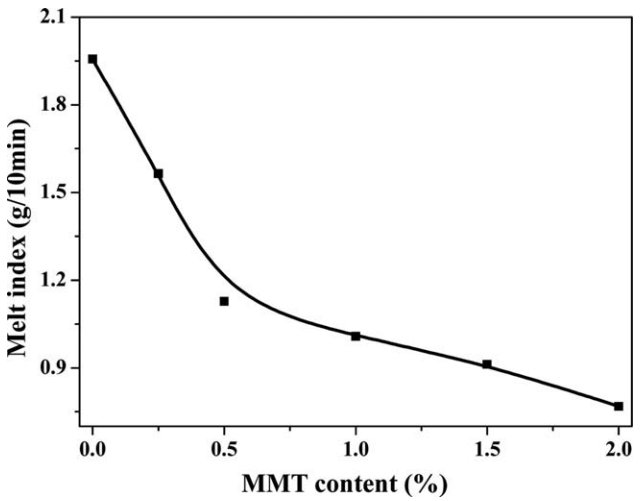

Figure 9. Melt index for PVA/MMT composites with different content of MMT.

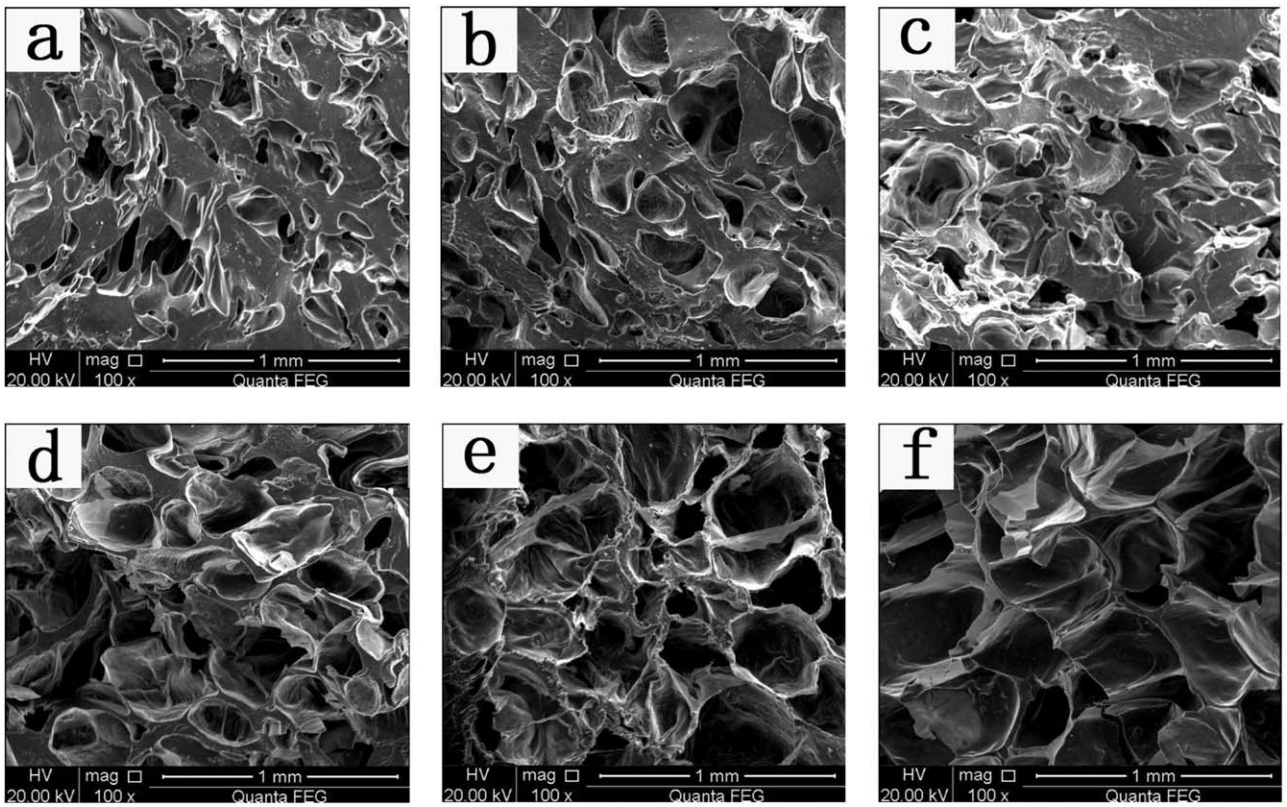

Figure 10. Cell morphology of PVA/MMT composite foams. MMT content: (a) 0 wt %, (b) 0.25 wt %, (c) 0.5 wt %, (d) 1.0 wt %, (e) 1.5 wt %, and (f) 2.0 wt %.

cell coalescence and rupture would be limited, leading to the improved foam morphology.

Another reason for the improved cell morphology would be ascribed to the decreased crystallization time of PVA in the presence of MMT. As discussed above, with the increase of MMT, Z_c increased and $t_{1/2}$ decreased, indicating the rapid crystallization. As a result, the generated bubble had no enough time to expand, resulting in reduced cell wall sharing and cell rupture. For example, with 2 wt % MMT, homogeneous cells with 300 μm aperture size were formed and the foam had close structure with little cell rupture, as shown in Figure 10(f).

Density of PVA/MMT Composite Foams

The dependence of density of PVA/MMT composite foams on MMT content is shown in Figure 11. With less than 0.25 wt % MMT, the foam density was close to bulk PVA (1.20 g/cm^3), because of the serious cell coalescence and rupture resulted by the low melt strength of PVA. With the increase of MMT, the density of the foams decreased quickly from 1.11 g/cm^3 of neat PVA foam to 0.35 g/cm^3 with 2 wt % MMT. MMT clays facilitated the foaming processing, leading to lower cell coalescence and rupture, as well as improved foaming ratio. Therefore, the

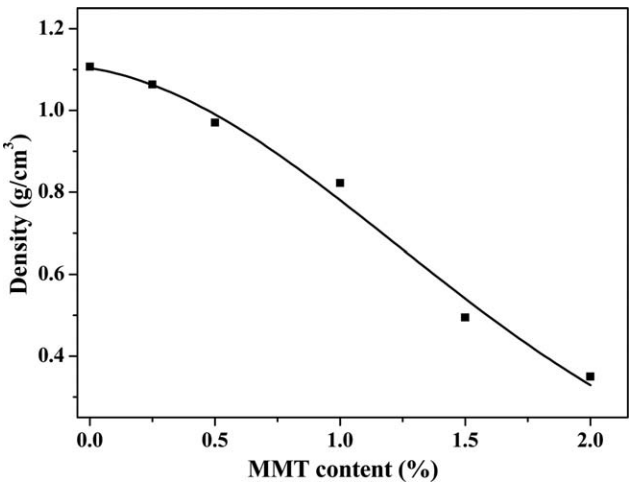

Figure 11. Density of PVA/MMT composite foams.

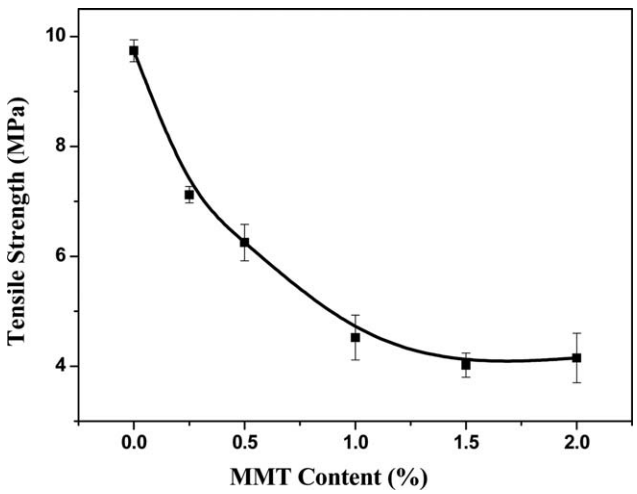

Figure 12. Mechanical properties of PVA/MMT composite foams.

density of the composite foams decreased dramatically although the density of MMT is higher than PVA.

Mechanical Properties

The mechanical properties of PVA and PVA/MMT composite foams are shown in Figure 12. The tensile strength decreased quickly from 9.97 MPa of neat PVA foam to 4.53 MPa of foam with less than 1 wt % MMT. With further increase of MMT (more than 1 wt %), the variation of tensile strength was little.

The reason for the change of strength of the foams could be explained through four aspects: (1) MMT could facilitate the foaming process, resulting in the decreased foaming density and thinner cell wall, leading to the decreased tensile strength. (2) Although the foaming density and the thickness of cell wall decreased, the cell size became uniform which reduced the stress concentration points. (3) As the reinforcing filler, MMT nanolayers could enhance the strength of PVA matrix as indicated by the increase of storage modulus. (4) The degree of crystallization of PVA/MMT composites would increase the strength of the matrix. Therefore, taking all these factors, the tensile strength did not decreased as the density but exhibited a plateau of approximately 4.53 MPa for composite foams with 1–2 wt % MMT content.

CONCLUSIONS

Novel PVA/intercalated MMT nanocomposite foams were fabricated by melt extrusion process. The effect of MMT content on the structure and properties of the resulting foams were investigated. The results revealed that pristine MMT could be intercalated by PVA during melt-extrusion. Both exfoliation and intercalation structure was formed in the composites. MMT might act as nucleating agent and induce the crystallization of PVA. The crystallization time reduced with the increase of MMT. The strong interaction between PVA and MMT restricted the motion of PVA molecules, leading to the enhanced complex viscosity, storage modulus, and melt flow index, which resulted in the improved melt elasticity and melt strength. With the increase of MMT, the cell coalescence and rupture of the composite foams decreased. The cell wall became thinner and the cell size distribution became more uniform. The density of the foams decreased from 1.11 g/cm^3 of neat PVA foam to 0.35 g/cm^3 of foams with 2 wt % MMT, which could be attributed to the enhanced melt strength and the reduced crystallization time. With the increase of MMT, the tensile strength of PVA/MMT foams decreased because of the enlarged foaming ratio and decreased density. Also MMT could reinforce PVA matrix, resulting in the stable tensile strength of composite foams with the increase of MMT. The PVA/MMT foams prepared by the novel, efficient, and economic processing method possess good performance and would have a wide application prospects in packaging, water treatment, heat/sound insulation, which may replace the nondegradable polystyrene and polyethylene foams.

ACKNOWLEDGMENTS

This work was supported by the National Natural Science Foundation of China (51373004 and 51203004), Beijing Natural Science Foundation (2122014), the Scientific and Technological Development Project of Beijing Municipal Commission of Education (KM201310011001), Youth Elite Project of Beijing Colleges (YETP1453), Innovation Ability Promotion Plan of Beijing Municipal Commission of Education (PXM2013_014213_000097), Beijing Top Young Innovative Talents Program (2014000026833ZK13), and Funding of Key Laboratory of Carbohydrate and Biotechnology Ministry of Education (KLCCB-KF201201).

REFERENCES

1. Lee, S. T.; Ramesh, N. S. Polymeric Foams Mechanisms and Materials; CRC Press INC: Boca Raton, **2004**.
2. Debiagi, F.; Marim, B. M.; Mali, S. *J. Polym. Environ.* **2015**, *23*, 269.
3. Liu, D.; Zhu, C.; Peng, K.; Guo, Y.; Chang, P. R.; Cao, X. F. *Ind. Eng. Chem. Res.* **2013**, *52*, 6177.
4. Chen, N.; Zhang, J. *Chn. J. Polym. Sci.* **2010**, *28*, 903.
5. Li, Y.; Wu, W.; Lin, F.; Xiang, A. *J. Appl. Polym. Sci.* **2012**, *126*, 162.
6. Finch, C. A. Polyvinyl Alcohol Developments; Wiley: New York, **1991**.
7. Jiang, X.; Tan, B.; Zhang, X.; Ye, D.; Dai, H.; Zhang, X. *J. Appl. Polym. Sci.* **2012**, *125*, 697.
8. Jang, J.; Lee, D. *Polymer* **2003**, *44*, 8139.
9. Bai, X.; Ye, Z.; Li, Y.; Zhou, L.; Yang, L. *Process. Biochem.* **2010**, *45*, 60.
10. Preechawong, D.; Peesan, M.; Rujiravanit, R.; Supaphol, P. *Macromol. Symp.* **2004**, *216*, 217.
11. Ramesh, N. S.; Malwitz, N. Extrusion of novel water soluble biodegradable foams. In: Annual Technical Conference, Conference Proceedings, Boston, **1995**; p 2171.
12. Yeh, J.; Xu, P.; Tsai, F. *J. Mater. Sci.* **2007**, *42*, 6590.
13. Bee, S.; Ratnam, C.; Sin, L.; Tee, T.; Hui, D.; Kadhum, A.; Rahmat, A.; Lau, J. *Compos. Part B Eng.* **2014**, *63*, 141.
14. Soulestin, J.; Rashmi, B.; Bourbigot, S.; Lacrampe, M.; Krawczak, P. *Macromol. Mater. Eng.* **2012**, *297*, 444.
15. Yu, Y.; Lin, C.; Yeh, J.; Lin, W. *Polymer* **2003**, *44*, 3553.
16. Majdzadeh-Ardakani, K.; Nazari, B. *Compos. Sci. Technol.* **2010**, *70*, 1557.
17. Paranhos, C.; Soares, B.; Oliveira, R.; Pessan, L. *Macromol. Mater. Eng.* **2007**, *292*, 620.
18. Dean, K.; Do, M.; Petinakis, E.; Yu, L. *Compos. Sci. Technol.* **2008**, *68*, 1453.
19. Wu, W.; Tian, H.; Xiang, A. *J. Polym. Environ.* **2012**, *20*, 63.
20. Lin, F.; Wu, W.; Sun, H.; Xiang, A. *J. Polym. Mater.* **2011**, *28*, 577.
21. Avrami, M. *J. Chem. Phys.* **1939**, *7*, 1103.
22. Bianchi, O.; Oliveira, R.; Fiorio, R.; Martins, J.; Zattera, A.; Canto, L. *Polym. Test.* **2008**, *27*, 722.
23. Schlund, B.; Utracki, L. A. *Polym. Eng. Sci.* **1987**, *27*, 1523.